Correction of Misalignment Artifacts Among 2-D Cardiac MR Images in 3-D Space

Joel Barajas[1,2], Karla L. Caballero[1], Jaume Garcia Barnés[1], Francesc Carreras[3], Sandra Pujadas[3], and Petia Radeva[1]

[1] Computer Vision Center, UAB Bellaterra Barcelona 08193, Spain,
[2] CICATA-IPN, Queretaro, Mexico,
[3] Hospital de la Sta Creu i St Pau, Barcelona, Spain
joel.barajas@cvc.uab.es

Abstract. Cardiac Magnetic Resonance images offer the opportunity to study the heart in detail. One of the main issues in its modelling is to create an accurate 3-D reconstruction of the left ventricle from 2-D views. A first step to achieve this goal is the correct registration among the different image planes due to patient movements. In this article, we present an accurate method to correct displacement artifacts using the Normalized Mutual Information. Here, the image views are treated as planes in order to diminish the approximation error caused by the association of a certain thickness, and moved simultaneously to avoid any kind of bias in the alignment process. This method has been validated using real and syntectic plane displacements, yielding promising results.

1 Introduction

Cardiac diseases have become one of the most common causes of death in recent years. Magnetic Resonance (MR) images from the heart provide an opportunity to study the anatomy and functions of the heart *in vivo*. As a result, it is becoming a widely used clinical tool to elaborate an accurate diagnosis. Many approaches have been developed to estimate the motion of the left ventricle, which are based on the initialization of a 3-D model and its deformation[1]. Then, it is required a good correspondence between the image planes in the space to achieve a proper description of the left ventricle volume[2].

A typical imaging session is composed of a number of imaging captures. Here, the required views are acquired during different breath holds. A necessary assumption to reconstruct a 3D model is to consider all the views as *instantly acquired*. As a result, a potential patient movement and a displacement of the left ventricle due to respiration can lead to misalignment artifacts[7]. Although some researchers have claimed that the development of more powerful and faster scanners skips the problem[4], this issue has still relevance in many clinical studies.

Some approaches have been proposed to solve the problem. One of them is a method based on registering a 3-D volume with sagittal and axial images as a preprocessing step to build a high resolution dynamic heart model from coronal slices[8]. Here, a line-by-line mean square difference is minimized. In same direction, Lötjönen *et al.*[5] have proposed the registration of a 3-D volume by the use of the Normal Mutual Information (NMI)[9]. They treat the images pixels as voxels by assigning a thickness equal to the slice separation between parallel short axis (SA) planes, and interpolating the voxel size using nearest neighbor in long axis (LA) views. However, it introduces some errors to

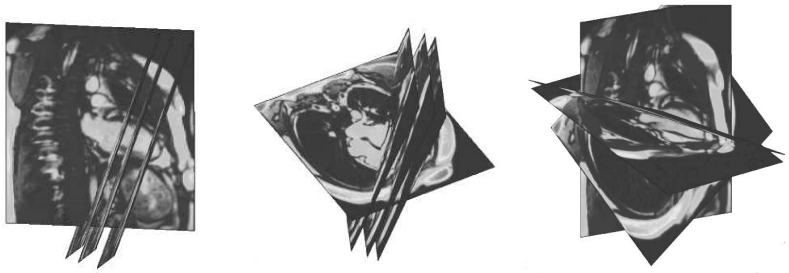

(a) (b) (c)

Fig. 1. Example of intersections among planes. (a) One LA plane vs three parallel SA. (b) A different LA view where both ventricles are observed vs three SA. (c) Four intersected LA planes used for one study

the analysis due to the approximation. It is because there could be a gap of up to 15mm considering 6 SA views, and taking into account that the thickness of the myocardium is no more than 12mm, this assumption becomes important. An alternative option could be to treat the thickness of the frame as it is reported by the image acquisition, but in order to achieve a good image quality it should be no less than 6mm which is still significant. Additionally, the proposed optimization method suggests the movement of a randomly chosen slice in the direction of its gradient and maximizing its NMI,which causes a bias depending on the slice. Moreover, this method use a constant step size of the movement which can provoke a uncertainty of when it has arrived to a maximum besides the slow convergence.

In this paper, we propose an alternative solution to the problem of misaligned MR images in a 3-D reconstruction of the left ventricle, by treating the MR images as planes on the space, and using the NMI as a measure of registration which is maximized using the steepest descendent method. In figure 1 typical intersections among planes of a given patient are shown. We suggest to use the intersection line between a given SA plane and an intersecting LA one, sample it, and extract the gray values associated with this points in both images. Then the NMI is estimated for these values generating an alignment measure. Thus, all of NMI values obtained from the intersections between the SA and LA views are combined to generate a global measure of alignment. Later, all of the images are moved simultaneously in order to arrive to a maximum by the steepest descendent method using a non constant step size. Finally, some results, discussion and conclusion are presented.

2 Methods

2.1 Planes Intersection

Having a SA MR image and a LA MR image, it is possible to obtain their spatial information from the DICOM headers respect to a common coordinate system, allowing the estimation of geometrical correspondences among all the views. A translation of the initial corner of the image, two orientation vectors, and an scale factor to convert pixels into millimeters are stored automatically. Hence, the equation of each of the image plane can be calculated.

Let I_{SA_i} be a short axis plane i of a total of N short axis planes, and I_{LA_j} be a long axis plane j of a total of M long axis planes, thus there exist a line intersection, $\mathbf{L_{ij}}$, between them which can be obtained from their plane equations by finding 2 points of this line. It can be expressed as: $\mathbf{L}_{ij} = \mathbf{r}_0 + t\mathbf{w}$,

where $\mathbf{r}_0$ is a point on the line, t is a free parameter, and $\mathbf{w}$ is a unitary vector parallel to the line. In order to find the pixel values along $\mathbf{L}_{ij}$ on I_{SA_i} and I_{LA_j}, it has to be placed on each of the image spaces. Thus, a point $\mathbf{p}_{L_{ij}} = \mathbf{L}_{ij}(t_0)$ can be expressed on the image spaces $\mathbf{p}_{SA_i} \in U_{SA_i}$ and $\mathbf{p}_{LA_j} \in U_{LA_j}$, from the image plane I_{SA_i} and I_{LA_j} respectively, as follows:

$$\mathbf{p}_{SA_i} = \left[\mathbf{R}_x^{SA_i}\mathbf{R}_y^{SA_i}\mathbf{R}_z^{SA_i}\right]^{-1}\left(\mathbf{p}_{L_{ij}} - \mathbf{O}_{SA_i}\right), \tag{1}$$

$$\mathbf{p}_{LA_j} = \left[\mathbf{R}_x^{LA_j}\mathbf{R}_y^{LA_j}\mathbf{R}_z^{LA_j}\right]^{-1}\left(\mathbf{p}_{L_{ij}} - \mathbf{O}_{LA_j}\right), \tag{2}$$

where $\mathbf{R}_x^{SA_i}$,$\mathbf{R}_y^{SA_i}$,$\mathbf{R}_z^{SA_i}$, are the direction of the x-axis, y-axis, and z-axis of U_{SA_i} respectively, while $\mathbf{O}_{SA_i}$ is a translation of the initial corner of I_{SA_i}. In the same manner, $\mathbf{R}_x^{LA_j}$,$\mathbf{R}_y^{LA_j}$,$\mathbf{R}_z^{LA_j}$ and $\mathbf{O}_{LA_j}$, are the descriptors of the space U_{LA_j}. Here the points $\mathbf{p}_{SA_i}$ and $\mathbf{p}_{LA_j}$ are in $\mathbb{R}^3$. However, since these points lie on $\mathbf{L_{ij}}$, the z-coordinate is equal to zero. Hence, after reducing the dimensionality of the points to $\mathbb{R}^2$ and applying a scale factor, these points can be expressed in pixels in U_{SA_i} and U_{LA_j} respectively.

Therefore, by applying the equations 1 and 2, a pair of gray values can be obtained for a single point $\mathbf{p}_{L_{ij}}$ coming from each of the images planes I_{SA_i} and I_{LA_j}, at the points $\mathbf{p}_{SA_i}$ and $\mathbf{p}_{LA_j}$ respectively.

Once the intersection line has been estimated, the image ranges are intersected, and the resulting line segment is sampled to generate a fixed number of points $\mathbf{p}_{L_{ij}}$. By using the equations 1 and 2, the points on I_{SA_i} and I_{LA_j} can be found. However, the corresponding gray values are only available for integer values of $\mathbf{p}_{SA_i}$ and $\mathbf{p}_{LA_j}$. We have observed that typically the myocardium in the SA and LA views have a thickness of 4-6 pixels (7.9-11.9mm), which means that a simple rounding of $\mathbf{p}_{SA_i}$ and $\mathbf{p}_{LA_j}$ is not suitable. Hence, we have performed a linear interpolation of the gray values along the sampled line so that $\mathbf{v}_{SA_i}$ and $\mathbf{v}_{LA_j}$ approximate continuous lines with reliable image values. To avoid any kind of bias, the sampling process has been designed using the parameter t so as to have the same points regardless of the order.

2.2 Correspondence Measure

Having $\mathbf{v}_{SA_i}$ and $\mathbf{v}_{LA_j}$, the problem turns to be a registration issue with two gray value vectors available. Thus, the Normalized Mutual Information (NMI)[9] has been employed to measure the correspondence between $\mathbf{v}_{SA_i}$ and $\mathbf{v}_{LA_j}$, and, as a result, between I_{SA_i} and I_{LA_j}. The NMI, S, is defined as:

$$S(\mathbf{v}_{SA_i}, \mathbf{v}_{LA_j}) = \frac{H(\mathbf{v}_{SA_i}) + H(\mathbf{v}_{LA_j})}{H(\mathbf{v}_{SA_i}, \mathbf{v}_{LA_j})}, \tag{3}$$

where $H(\mathbf{v}_{SA_i})$ and $H(\mathbf{v}_{LA_j})$ are the marginal entropies of $\mathbf{v}_{SA_i}$ and $\mathbf{v}_{LA_j}$ respectively, and $H(\mathbf{v}_{SA_i}, \mathbf{v}_{LA_j})$ is the joint entropy of both vectors. To calculate the probability distribution of $\mathbf{v}_{SA_i}$,$\mathbf{v}_{LA_j}$, and their joint probability, the number of bins has been adjusted according to the number of samples of the intersection vectors. It is mainly because the gray values in a given $\mathbf{v_x}$ can vary until thousands, and by selecting a region of interest, the variety of gray values can be little, which allows some bins to be 1 or 2 undermining the measure. Thus, the number of bins has been established to be 20-40 based on the number of samples. In addition, a preprocessing step has been performed to the images available. Here, the logarithmic of the image is computed, which improves the gray distribution and compresses its range[3]. Because the sampling process

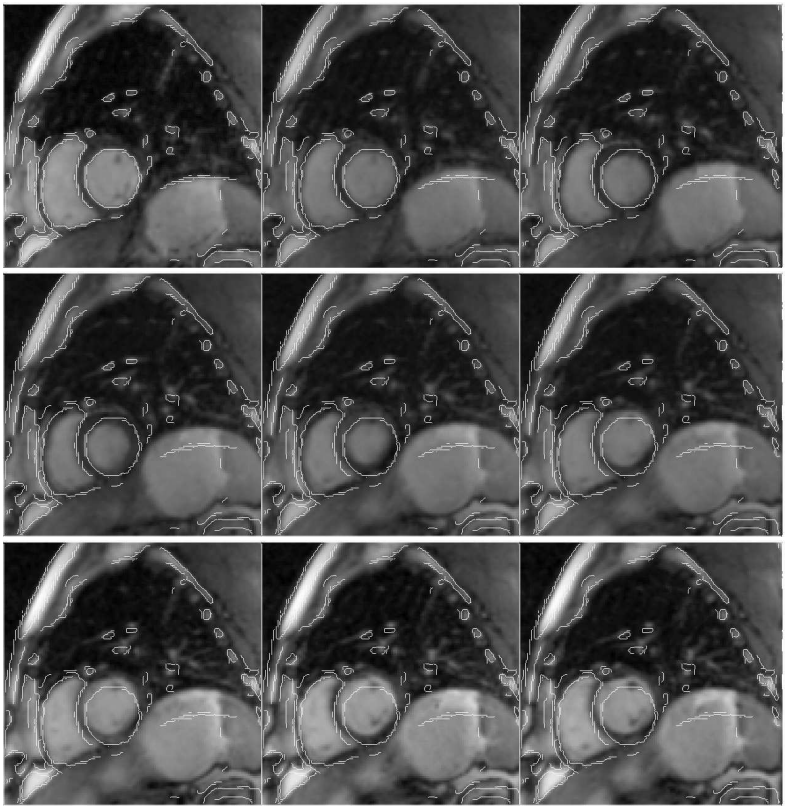

Fig. 2. From left to right and from top to bottom, a cardiac cycle sequence from a patient with the motion artifact due to respiration. The contours of the first frame have been added for better visualization

assures the selection of the same points regardless the order, it is guaranteed that:

$$S(\mathbf{v}_{SA_i}, \mathbf{v}_{LA_j}) = S(\mathbf{v}_{LA_j}, \mathbf{v}_{SA_i}).$$

2.3 Misalignment Correction

One of the main causes of misalignment among MR image planes is respiration[7]. During an imaging session, the patient is asked to hold the breath while the images are acquired. Long periods of time, up to 20 seconds, provoke the patient to inhale small quantities of air which cause a certain movement of the heart. We have performed an experiment where a patient is scanned while this effect is introduce during a cardiac cycle. It is shown in the figure 2. It can be observed that there is a certain level of rotation. Nonetheless, the left ventricular motion can be assumed to be a translation. Thus, we have selected a region of interest which contains the myocardium, and tried to fit the image planes by translations, since we are interested in the left ventricle.

The movement artifacts can also be observed from the intersection vectors $\mathbf{v}_{LA_j}$ and $\mathbf{v}_{SA_i}$. As an example, in the figure 3 a typical misalignment artifact is shown. Since we are interested on the analysis of the left ventricle, we have selected a region of interest where the left ventricle is appreciated. Although the problem can be treated as moving one plane until $S(\mathbf{v}_{SA_i}, \mathbf{v}_{LA_j})$ is maximum and repeating the process until it converges for all the N short axis and M long axis planes, the main drawback of this is that a movement in one SA plane,

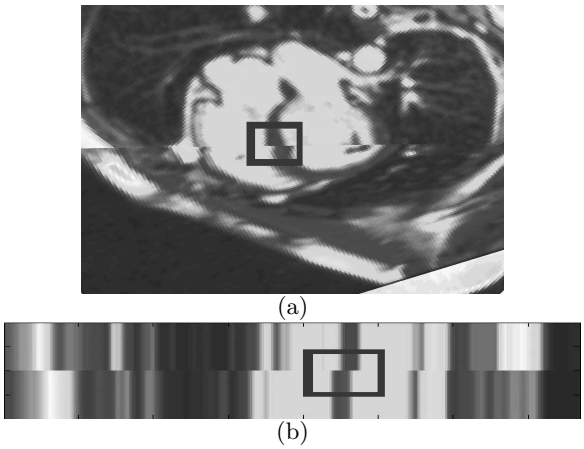

Fig. 3. Example of misalignment between a SA plane and a LA one. The square area represent the interventricular septum. (a) The SA and LA images in a common 3-D space. (b) The intersection vectors displayed one against the other.

affects the alignment with the other LA planes which intersect it. Consequently, we have designed a method to correct misalignments among the image planes by moving all the planes simultaneously.

We have calculated a global measure of alignment C to be maximized in this registration problem. A simple approach is to use the mean of $S(\mathbf{v}_{SA_i}, \mathbf{v}_{LA_j})$ for all the intersections between the N SA views and the M LA ones. However, because of the NMI probabilistic properties, it has been designed C to be the mean of the $S(\mathbf{U}_{SA_i}, \mathbf{U}_{LA})$ and $S(\mathbf{U}_{LA_j}, \mathbf{U}_{SA})$ for all SA planes i and LA planes j, where $\mathbf{U}_{SA_i} = \left[\mathbf{v}^T_{SA_{i1}}, \mathbf{v}^T_{SA_{i2}}, \ldots, \mathbf{v}^T_{SA_{iM}}\right]$ and $\mathbf{U}_{LA} = \left[\mathbf{v}^T_{LA_{i1}}, \mathbf{v}^T_{LA_{i2}}, \ldots, \mathbf{v}^T_{LA_{iM}}\right]$. Here $\mathbf{v}_{SA_{ij}}$ and $\mathbf{v}_{LA_{ij}}$ represent the intersection vectors $\mathbf{v}_{SA_i}$ of the SA view i with the LA one j, and the same for the LA view. Thus, we have estimated the NMI for all the intersections for a given plane, and computed the mean for all the planes.

There is a translation $\mathbf{O}_x$ of each of the image planes in a common space of dimension 3. If $\mathbf{d} = \left[\mathbf{O}^T_{SA_2}, \mathbf{O}^T_{SA_3}, \ldots, \mathbf{O}^T_{SA_N}, \mathbf{O}^T_{LA_1}, \mathbf{O}^T_{LA_2}, \ldots, \mathbf{O}^T_{SA_M}\right]$, it can be said that $C = F(\mathbf{d})$, where $\mathbf{d} \in \mathbb{R}^{3(N+M-1)}$. Therefore an optimization method can be applied to maximize C so as to find the best fitting of the image planes.

In order to maximize C, we have used the steepest descent method exposed in [6]. The gradient, ∇C, respect to $\mathbf{d}$ is estimated using finite differences by the central-difference equation of order $\mathbf{O}(h^2)$ for each dimension. Because of the definition of C, the implementation of ∇C can be simplified by finding $\mathbf{U}_{SA_{ij}}$ and $\mathbf{U}_{LA_{ij}}$ just for the intersection planes where d_k belongs to. Thus, the iteration of $\mathbf{d}$ is constrained along the line $\mathbf{d}_{k+1} = \mathbf{d}_k + \gamma \mathbf{g}_k$ where $\mathbf{g}_k$ is the direction of ∇C_k. Here, the step size γ is found from a single parameter maximization of $\phi(\gamma) = F(\mathbf{d}_k + \gamma \mathbf{g}_k)$. We have designed γ to be increased each time when C tends to be a local maximum and, by solving the single parameter maximization of $\phi(\gamma)$, C could be attracted to a higher maximum. If γ returns to the same value range in spite of the perturbation, the algorithm is left to converge to this maximum.

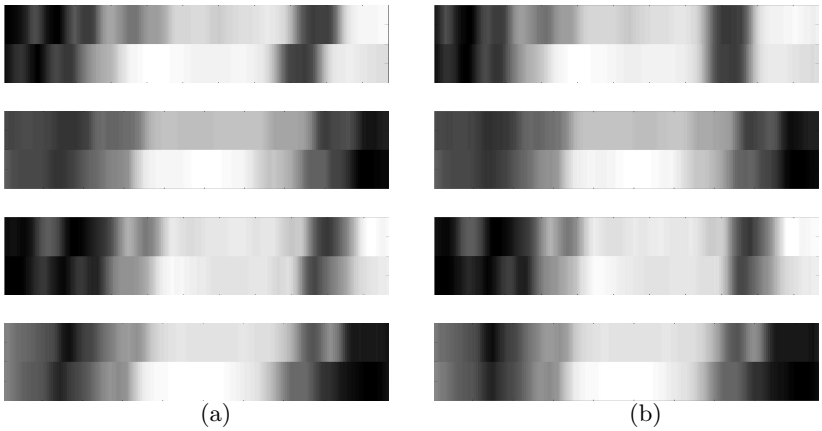

(a) (b)

Fig. 4. Some of the most significant misalignment artifacts in a real patient and the alignment performed by the proposed framework are shown. (a) Intersection vectors as acquired from the imaging session. (b) Misalignment artifacts corrected by our method.

3 Results

We have tested the proposed framework with a set of 12 healthy patients. Each case is composed of 7 parallel SA views from base to apex, and 4 LA views. In 3 of these views both ventricles are shown, and in the remaining 1 just the left ventricle is observed. The pixel spacing is 1.98 by 1.98mm for SA and 1.77 by 1.77mm for LA. The slice thickness is 8mm for SA and 6mm for LA. It is selected a region of interest in a SA view, and applied our framework to this region, which is propagated to the other SA planes.

We have applied our method in patients where movement artifacts have been observed by inspecting the intersection vectors. Then, some qualitative results are shown in figure 4 for one real case whose plane intersections are displayed in figure 1. Here some of the intersection vectors are shown before and after the alignment, showing a good registration between them. It should be noticed that all the planes have been moved simultaneously until a global fitting is achieved.

However, the performance of our framework can not be evaluated with the data from real patients due to the lack of the ground-truth, *i.e.* the movements during the imaging session. In order to overcome this problem, we have chosen one real patient, aligned it, and moved each of the planes by a random number from a given range. Even though there is a propagated error, it provides a good evaluation of our method. Thus, we have selected the patient exposed in the figure 4 to be move by 10 iterations at different displacement ranges. Then, each slice is moved along the three axis by an random number. The results of this experiment are shown in tables 1 and 2. Here, it can be observed that when the induced displacement increases, the error increases as well. It is mainly because the plane could be out of the myocardial region. However, it should be noted that these errors are smaller than a pixel (1.98mm), which in terms of the myocardial thickness (12mm) represents an accuracy of 87%.

4 Conclusion and Discussion

A method to register LA and SA MR images by eliminating the misalignment artifact has been proposed. There has not been introduced any kind of bias in

the movement behavior of the image slices, since these have been performed in the same global coordinate system instead of the left ventricle main axis. The image views have been treated as planes without thickness, which reduces the error of approximation that is significant for this case. It is because the myocardium could be represented by 4-6 pixels (7.9-11.9 mm) on the SA planes, while the slice thickness should not be less than 7 mm to achieve a good image equality. In addition, by treating the image data as voxels, some gaps between the SA planes are allowed, which introduce an error due to the interpolation between them, and hide part of the misalignment artifacts. Moreover, a minimum number of slice views are needed to register the image data using this idea which is not a requirement in our framework.

By inspecting the behavior of the alignment measure and the intersection vectors, it has been detected that there are more than one solution to the problem. It has been found good correspondences among the LA and SA slices at different locations, which suggests a number of displacement solutions. It is because, some regions of the myocardium are uniform allowing a plane to move freely inside them. On the other hand, there are some regions near to the apex where an acceptable solution tends to be an exact displacement, particularly when the right ventricle is not appreciated.

Additionally, it has been observed that the misalignment artifact is an important issue in the 3-D volume reconstruction task of the left ventricle. A high percentage of patients, 75%, has been identified with some level of movement. The inclusion of a rotation factor could help in the improvement of our registration method since the diaphragm provokes an orientation change in the image. However, this factor is not too significant when only the left ventricle is interested as it is the case.

Acknowledgments

This work is supported in part by a research grant of the *Instituto de la Salud Carlos III*, FIS: 04/2663, and by the Spanish Ministry of Education and Sciences (MEC) under the FPU grant Ref: AP2005-0926.

References

1. Alejandro F. Frangi, Wiro J. Niessen, and Max A. Viergever. Three-dimensional modeling for functional analysis of cardiac images: A review. *IEEE Trans. Med. Imaging*, 20(1):2–5, 2001.
2. Alejandro F. Frangi, Daniel Rueckert, Julia A. Schnabel, and Wiro J. Niessen. Automatic Construction of Multiple-object Three-dimensional Statistical Shape Models: Application to Cardiac Modelling. *IEEE Trans. Med. Imaging*, 21(9):1151–1166, 2002.

Table 1. Mean Displacement Error in milimeters for each XYZ coordinate in different movement ranges in the LA Slices

Range	X	Y	Z
$\pm 3mm$	0.5018 ± 0.2597	0.4653 ± 0.2028	0.4650 ± 0.1985
$\pm 4mm$	0.8790 ± 0.4373	1.0790 ± 0.3603	0.8199 ± 0.3725
$\pm 5mm$	1.0590 ± 0.4339	0.8545 ± 0.4540	0.6827 ± 0.2169
$\pm 6mm$	1.5728 ± 0.5630	1.3308 ± 0.4575	0.9359 ± 0.3711
$\pm 7mm$	1.5337 ± 0.5840	1.5227 ± 0.7223	1.8049 ± 0.8195

Table 2. Mean Displacement Error in milimeters for each XYZ coordinate in different movement ranges in the SA Slices

Range	X	Y	Z
$\pm 3mm$	0.5359 ± 0.2402	0.2776 ± 0.1412	0.4599 ± 0.1731
$\pm 4mm$	0.6415 ± 0.3420	0.7213 ± 0.3287	0.6814 ± 0.3035
$\pm 5mm$	0.7910 ± 0.3428	1.1546 ± 0.3356	0.6610 ± 0.3229
$\pm 6mm$	0.7004 ± 0.2197	1.0097 ± 0.4079	0.9686 ± 0.3285
$\pm 7mm$	1.5810 ± 0.4263	1.4611 ± 0.5188	1.1102 ± 0.3631

3. R. Gonzalez and R. Woods. *Image Processing*. Adison-Wesley, 1992.
4. M.R. Kaus, J. von Berg, J. Weese, W.J. Niessen, and V. Pekar. Automated Segmentation of the Left Ventricle in Cardiac MRI. *Medical Image Analysis*, 8(3):245–254, 2004.
5. Jyrki Lötjönen, Mika Pollari, Sari Kivistö, and Kirsi Lauerma. Correction of Movement Artifacts from 4-D Cardiac Short and Long-Axis MR Data. In Christian Barillot, David R. Haynor, and Pierre Hellier, editors, *MICCAI (2)*, volume 3217 of *Lecture Notes in Computer Science*, pages 405–412. Springer, 2004.
6. J. Mathews. *Numerical Methods for Science and Egineering*. Prentice Hall, 1992.
7. K. McLeish, D. L. G. Hill, D. Atkinson, J. M. Blackall, and R. Razavi. A study of the motion and deformation of the heart due to respiration. *IEEE Trans. Med. Imaging*, 21(9):1142–1150, 2002.
8. John Moore, Maria Drangova, Marcin Wierzbicki, and Terry M. Peters. A high resolution dynamic heart model based on averaged mri data. In Randy E. Ellis and Terry M. Peters, editors, *MICCAI (1)*, volume 2878 of *Lecture Notes in Computer Science*, pages 549–555. Springer, 2003.
9. C. Studholme, D. L. G. Hill, and D. J. Hawkes. Automated three-dimensional registration of magnetic resonance and positron emission tomography brain images by multiresolution optimization of voxel similarity measures. *Medical Physics*, 24(1):25–35, Jan. 1997.